High-Energy Vacuum Birefringence and Dichroism in an Ultrastrong Laser Field

Sergey Bragin, Sebastian Meuren,* Christoph H. Keitel, and Antonino Di Piazza
Max-Planck-Institut für Kernphysik, Saupfercheckweg 1, D-69117 Heidelberg, Germany

(Received 6 July 2017; published 21 December 2017)

A long-standing prediction of quantum electrodynamics, yet to be experimentally observed, is the interaction between real photons in vacuum. As a consequence of this interaction, the vacuum is expected to become birefringent and dichroic if a strong laser field polarizes its virtual particle–antiparticle dipoles. Here, we derive how a generally polarized probe photon beam is influenced by both vacuum birefringence and dichroism in a strong linearly polarized plane-wave laser field. Furthermore, we consider an experimental scheme to measure these effects in the nonperturbative high-energy regime, where the Euler-Heisenberg approximation breaks down. By employing circularly polarized high-energy probe photons, as opposed to the conventionally considered linearly polarized ones, the feasibility of quantitatively confirming the prediction of nonlinear QED for vacuum birefringence at the 5σ confidence level on the time scale of a few days is demonstrated for upcoming 10 PW laser systems. Finally, dichroism and anomalous dispersion in vacuum are shown to be accessible at these facilities.

DOI: 10.1103/PhysRevLett.119.250403

In the realm of classical electrodynamics, the electromagnetic field experiences no self-interaction in vacuum [1]. According to quantum electrodynamics (QED), however, a finite photon-photon coupling is induced by the presence of virtual charged particles in the vacuum [2]. For low-frequency electromagnetic fields $F^{\mu\nu}$, such vacuum polarization effects are described by the Euler-Heisenberg Lagrangian density [3–6]. Below the QED critical field $E_{\mathrm{cr}} = m^2/|e| \approx 1.3\times 10^{18}$ V/m, low-frequency vacuum polarization effects are suppressed [7–12] and the density is given by

$$\mathcal{L}_{\mathrm{EM}} = -\mathcal{F} + \frac{\alpha}{90\pi E_{\mathrm{cr}}^2}(4\mathcal{F}^2 + 7\mathcal{G}^2) + \cdots, \tag{1}$$

where $\mathcal{F} = F_{\mu\nu}F^{\mu\nu}/4$ and $\mathcal{G} = \tilde{F}_{\mu\nu}F^{\mu\nu}/4$ are the electromagnetic field invariants [13].

The Euler-Heisenberg Lagrangian predicts that the vacuum resembles a birefringent medium [14–17]. The smallness of the QED prediction for the light-by-light scattering cross section in the low-energy regime opens up the possibility to search for physics beyond the standard model, e.g., axionlike or minicharged particles and paraphotons, by measuring optical vacuum polarization effects [18–22], see also [23,24].

Recent astronomical observations hint at the existence of vacuum birefringence [25] (see also the remarks in [26,27]). However, a direct laboratory-based verification of this fundamental property of the vacuum is still missing. Laboratory experiments like BFRT [28], BMV [29], PVLAS [30], and Q&A [31] have so far employed magnetic fields to polarize the vacuum and optical photons to probe it, though without reaching the required sensitivity.

The strongest electromagnetic fields of macroscopic extent are nowadays produced by lasers. However, even the intensities $I \sim 10^{23}$ W/cm^2 envisaged for future 10 PW-class optical lasers [32,33] are still well below the critical intensity $I_{\mathrm{cr}} = E_{\mathrm{cr}}^2 \approx 4.6\times 10^{29}$ W/cm^2. Therefore, the leading-order correction given in Eq. (1) is sufficient to describe low-frequency vacuum polarization effects. Recently, various setups have been considered to measure them [34–52], but all suggested experiments will remain challenging in the foreseeable future.

As the light-by-light scattering cross section attains its maximum at the pair-production threshold [2], it is natural to consider high-energy photons to probe vacuum birefringence [53–58]. A photon four-momentum q^μ ($q^0 = \omega$, $q^2 = 0$) allows us to construct a third invariant, the quantum nonlinearity parameter (see [2], § 101)

$$\chi = \frac{\sqrt{-(f^{\mu\nu}q_\nu)^2}}{E_{\mathrm{cr}}m} \approx 0.5741\frac{\omega}{\mathrm{GeV}}\sqrt{\frac{I}{10^{22}\ \mathrm{W/cm^2}}} \tag{2}$$

[for a plane-wave background field with amplitude $f^{\mu\nu}$ and phase-dependent pulse shape $\psi'(\phi)$, i.e., $F^{\mu\nu} = f^{\mu\nu}\psi'(\phi)$, details are given below; the last relation in Eq. (2) assumes a head-on collision]. As gamma photons with energies $\omega \gtrsim 1$ GeV are obtainable from Compton backscattering [2,59–62], the regime $\chi \sim 1$ is attainable in future laser-based vacuum birefringence experiments.

In the nonperturbative regime $\chi \gtrsim 1$, the Euler-Heisenberg approximation is no longer applicable, as it neglects the contribution of the probe photon momentum, which flows in the electron-positron loop [see Fig. 1(a)]. Instead, the polarization operator in the background field must be employed [see Fig. 1(b)]. For low-energy photons, both objects in Fig. 1 are related by functional derivatives [14]. The regime $\chi \gtrsim 1$ is qualitatively different from the

 © 2017 American Physical Society

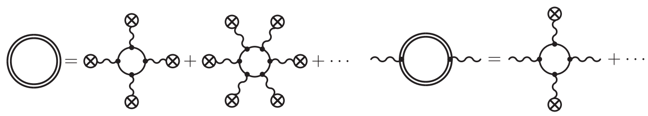

(a) Euler-Heisenberg (b) Polarization operator

FIG. 1. The Euler-Heisenberg effective action is only valid for approximately constant fields (denoted by a wiggly line with a cross). The polarization operator must be considered if the momentum of the probe photon (wiggly line) becomes influential ($\chi \gtrsim 1$). Here, a solid double line denotes the exact electron propagator inside a classical background field.

one where the Euler-Heisenberg approximation is valid, in particular, due to the following two reasons: (1) electron-positron photoproduction becomes sizable, and thus, the vacuum acquires dichroic properties; (2) the vacuum exhibits anomalous dispersion [11,56,63–65].

In this Letter, we put forward an experimental scheme to measure high-energy vacuum birefringence and dichroism in the nontrivial regime $\chi \gtrsim 1$. It is based on Compton backscattering to produce polarized gamma photons and exploits pair production in matter to determine the polarization state of the probe photon after it has interacted with a linearly polarized strong laser pulse. By analyzing the consecutive stages of this type of experiment, we show that for vacuum birefringence, the required measurement time is reduced by two orders of magnitude if a circularly polarized probe photon beam is employed (hitherto, only linearly polarized probe gamma photons have been considered for setups similar to ours [53–56,66]).

Assuming conservative experimental parameters, we demonstrate that with this type of setup and the observables we introduce [see Eq. (13)], the quantitative verification of the strong-field QED prediction for vacuum birefringence and dichroism is feasible with an average statistical significance of 5σ on the time scale of a few days at upcoming 10 PW laser facilities.

In the following, we consider a linearly polarized plane-wave laser pulse, described by the four-potential $A^\mu(kx) = a^\mu \psi(kx)$. Here, x^μ is the position four-vector, k^μ is a characteristic laser photon four-momentum ($k^0 = \omega_L$, $k^2 = 0$), a^μ characterizes the amplitude of the field ($a^2 < 0$, $ka = 0$, $f^{\mu\nu} = k^\mu a^\nu - k^\nu a^\mu$), and $\psi(kx)$ defines its pulse shape ($|\psi(kx)|, |\psi'(kx)| \lesssim 1$; a prime denotes the derivative of a function with respect to its argument).

A gauge- and Lorentz-invariant measure of the laser field strength is the classical intensity parameter [11]

$$\xi = \frac{|e|\sqrt{-a^2}}{m} \approx 0.7495 \frac{\mathrm{eV}}{\omega_L} \sqrt{\frac{I}{10^{18}\ \mathrm{W/cm^2}}}. \qquad (3)$$

Here, we focus on high-intensity optical lasers ($I \gtrsim 10^{20}\ \mathrm{W/cm^2}$, $\omega_L \sim 1$ eV), i.e., the regime $\xi \gg 1$.

Inside a plane-wave background field, an incoming external photon line (see Fig. 2) in a Feynman diagram corresponds (up to normalization) to the function $\Phi^\mu_q(x)$, which is a solution of the Dyson equation [2,67] with initial condition $\Phi^\mu_q(x) \to \Phi^{(0)\mu}_q(x) = \epsilon^{(0)\mu} e^{-iqx}$ as $kx \to -\infty$ ($\epsilon^{(0)}\epsilon^{(0)*} = -1$, $q\epsilon^{(0)} = 0$). After applying the local constant field approximation (valid if $\xi \gg 1$) and following [67], we find that to leading order, $\Phi^\mu_q(x)$ is given by (see also [18,56,64,65])

FIG. 2. A background field changes the photon dispersion relation via radiative corrections induced by virtual particles [2]. Here, we neglect higher-order radiative corrections to the electron-positron loop as $\alpha\chi^{2/3} \ll 1$ [11].

$$\Phi^\mu_q(x) = \epsilon^\mu(kx) e^{-iqx}, \qquad \epsilon^\mu(kx) = \sum_{i=1,2} c_i(kx) \Lambda^\mu_i, \qquad (4)$$

where

$$\epsilon^\mu(kx \to -\infty) = \epsilon^{(0)\mu} = \sum_{i=1,2} c_i^{(0)} \Lambda^\mu_i, \qquad (5)$$

and $\Lambda^\mu_1 = f^{\mu\nu} q_\nu / \sqrt{qf^2q}$, $\Lambda^\mu_2 = -\tilde{f}^{\mu\nu} q_\nu / \sqrt{qf^2q}$ ($q\Lambda_i = k\Lambda_i = 0$, $\Lambda_i \Lambda_j = -\delta_{ij}$; note that Λ^μ_2 is actually a pseudo four-vector) [67–69]. The coefficients $c_i(kx)$ and $c_i^{(0)}$ are connected via

$$c_i(kx) = c_i^{(0)} \exp[i\phi_i(kx) - \lambda_i(kx)], \qquad (6)$$

where

$$\begin{bmatrix} \phi_i(kx) \\ \lambda_i(kx) \end{bmatrix} = -\frac{1}{2kq} \int_{-\infty}^{kx} d\phi \begin{bmatrix} \mathrm{Re}[p_i(\phi,\chi)] \\ \mathrm{Im}[p_i(\phi,\chi)] \end{bmatrix}, \qquad (7)$$

[we refer to $\phi_i = \phi_i(kx \to \infty)$ as phase shifts and to $\lambda_i = \lambda_i(kx \to \infty)$ as decay parameters] with

$$\begin{bmatrix} p_1(kx,\chi) \\ p_2(kx,\chi) \end{bmatrix} = \frac{\alpha m^2}{3\pi} \int_{-1}^{+1} dv \begin{bmatrix} (w-1) \\ (w+2) \end{bmatrix} \frac{f'(u)}{u}, \qquad (8)$$

$w = 4/(1-v^2)$, $u = [w/\chi(kx)]^{2/3}$, $\chi(kx) = \chi|\psi'(kx)|$, and $f(u) = \pi[\mathrm{Gi}(u) + i\mathrm{Ai}(u)]$ [11,70].

In order to extend the above result from a single photon to a photon beam (which is, in general, not in a pure polarization state), we introduce the following density tensors, which describe the initial ($\varrho^{(0)\mu\nu}$) and the final ($\varrho^{\mu\nu}$) polarization state of the beam [2,71,72]

$$\varrho^{(0)\mu\nu} = \sum_a w_a \epsilon_a^{(0)\mu} \epsilon_a^{(0)*\nu} = \sum_{i,j=1,2} \rho_{ij}^{(0)} \Lambda^\mu_i \Lambda^\nu_j,$$
$$\varrho^{\mu\nu} = \sum_a w_a \epsilon_a^\mu \epsilon_a^{*\nu} = \sum_{i,j=1,2} \rho_{ij} \Lambda^\mu_i \Lambda^\nu_j. \qquad (9)$$

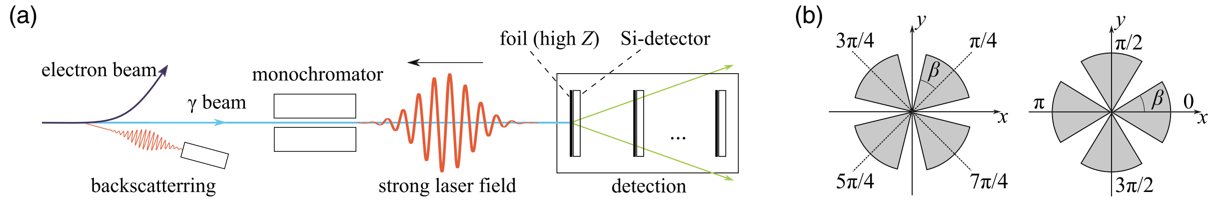

FIG. 3. (a) Experimental setup. Polarized highly energetic gamma photons (produced via Compton backscattering) propagate through a strong laser field, which induces vacuum birefringence and dichroism. Afterward, the gamma photons are converted into electron-positron pairs. From their azimuthal distribution, the polarization state is deduced. (b) Regions of the transverse plane (gray), which are used to define the observables R_B (left) and R_D (right) [see Eq. (13)].

Here, w_a represents the probability to find a photon with polarization four-vector $\epsilon_a^{(0)\mu}$ (ϵ_a^{μ}) in the initial (final) beam.

Using the identity matrix I and the Pauli matrices $\boldsymbol{\sigma} = (\sigma_1, \sigma_2, \sigma_3)$ [2], we expand the initial ($\rho_{ij}^{(0)}$) and the final (ρ_{ij}) polarization density matrices as [2,71,72]

$$\rho^{(0)} = \frac{1}{2}(S_0^{(0)}\mathrm{I} + \mathbf{S}^{(0)}\boldsymbol{\sigma}), \qquad \rho = \frac{1}{2}(S_0\mathrm{I} + \mathbf{S}\boldsymbol{\sigma}) \tag{10}$$

[$\mathrm{Tr}(\rho^{(0)}) = S_0^{(0)}$, $\mathrm{Tr}(\rho) = S_0$; $S_0 \le S_0^{(0)}$, in general, as the photons can decay in the strong background field].

The real Stokes parameters $S^{(0)} = \{S_0^{(0)}, \mathbf{S}^{(0)}\}$ [$\mathbf{S}^{(0)} = (S_1^{(0)}, S_2^{(0)}, S_3^{(0)})$] and $S = \{S_0, \mathbf{S}\}$ [$\mathbf{S} = (S_1, S_2, S_3)$] completely characterize the initial (final) polarization state of the beam [72,73]. Therefore, the following relations describe any possible vacuum birefringence and/or dichroism experiment [see Eqs. (4), (6), (9), and (10)]

$$\begin{pmatrix} S_0 \\ S_3 \end{pmatrix} = e^{-(\lambda_1+\lambda_2)} \begin{pmatrix} \cosh\delta\lambda & \sinh\delta\lambda \\ \sinh\delta\lambda & \cosh\delta\lambda \end{pmatrix} \begin{pmatrix} S_0^{(0)} \\ S_3^{(0)} \end{pmatrix},$$
$$\begin{pmatrix} S_1 \\ S_2 \end{pmatrix} = e^{-(\lambda_1+\lambda_2)} \begin{pmatrix} \cos\delta\phi & -\sin\delta\phi \\ \sin\delta\phi & \cos\delta\phi \end{pmatrix} \begin{pmatrix} S_1^{(0)} \\ S_2^{(0)} \end{pmatrix}. \tag{11}$$

Here, $\delta\phi = \phi_2 - \phi_1$ is related to vacuum birefringence and $\delta\lambda = \lambda_2 - \lambda_1$ to vacuum dichroism.

In the following, we discuss possible high-energy vacuum birefringence and/or dichroism experiments [see Fig. 3(a)] at the Apollon facility (F1/F2 laser) [74], ELI-NP (two 10 PW lasers) [75,76], and ELI-Beamlines (ELI-BL; L3/L4 laser) [77]. At each facility, a 10 PW laser is employed to polarize the vacuum, and the second laser is utilized to produce electron bunches via laser wakefield acceleration [78,79]. We also consider a possible experiment (denoted as LINAC-L) at a conventional electron accelerator, e.g., the European XFEL [80], FACET-II [81], or SACLA [82], combined with a high-repetition (10 Hz) 1 PW laser. The parameters of the considered facilities are summarized in the Supplemental Material [83].

We assume that $N_e = 10^8$ monoenergetic few-GeV electrons are used in one experimental cycle for the generation of probe gamma photons via Compton backscattering.

For a rectangular pulse with N cycles $\{\psi'(kx) = \sin(kx)$ if $kx \in [-N\pi, N\pi]$ and $\psi'(kx) = 0$ otherwise$\}$, the relative phase shift $\delta\phi$ depends only on χ and ξN; it is plotted in Fig. 4. We conclude that $|\delta\phi| \lesssim 0.1$ for upcoming laser systems in the regime $0.1 \lesssim \chi < 1$, where a clean vacuum birefringence measurement is feasible as pair production is exponentially suppressed. Notably, the quantity $\delta\phi$ decreases with the increase of the probe photon energy for $\chi \gtrsim 2.5$, which characterizes the anomalous dispersion of the vacuum in this regime [11,56,63–65].

For obtaining better estimates as those given in Fig. 4, in the following, we employ a Gaussian pulse envelope $\psi'(kx) = \exp[-(kx/\Delta\phi)^2]\sin(kx)$, where $\Delta\phi$ is related to the duration of the pulse Δt (FWHM of the intensity) via $\Delta\phi = \omega_L \Delta t/\sqrt{2\ln 2}$. This pulse collides with $N_\gamma = N_e \sigma_{\mathrm{bs}}(I_{\mathrm{bs}}/\omega_{\mathrm{bs}})\Delta t_{\mathrm{bs}}$ gamma photons, where σ_{bs} is the cross section of Compton scattering [2], and the index "bs" indicates the parameters characterizing the backscattering process. To obtain a high degree of polarization, we consider only photons which are scattered in the region $\theta \in (0, \theta_{\max} \ll 1)$, where θ denotes the polar angle ($\theta = 0$ corresponds to perfect backscattering) [2,59–62,83].

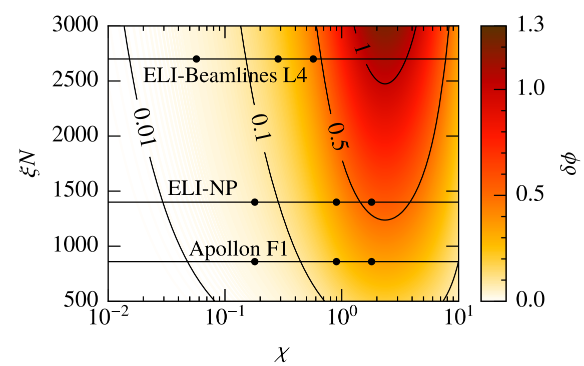

FIG. 4. Plot of $\delta\phi$ as a function of χ and ξN for a rectangular pulse profile. For each of the three laser facilities, gamma photons with energy $\omega = 0.1$ GeV (left point), $\omega = 0.5$ GeV (central point), and $\omega = 1$ GeV (right point) are indicated. Note that $|\delta\phi| \gtrsim 0.1$ is also achievable by employing a longer PW laser pulse (e.g., National Ignition Facility with $\Delta t = 3$ ns [32]) and probe photons with $\omega \gtrsim 0.1$ GeV.

Below, we employ $\Delta t_{bs} = \Delta t$, $\omega_{bs} = 1.55$ eV, and $I_{bs} = 4.3 \times 10^{16}$ W/cm^2 [considering linear Compton scattering is sufficient as $\xi_{bs} = 0.1$ for this laser; see Eq. (3)].

One of the main experimental challenges is to analyze the final polarization state of the gamma photons. Here, we consider pair production in a screened Coulomb field of charge $Z|e|$ [91–94]. The spin-summed pair production cross section is given by

$$d\sigma_{pp} = \frac{d\varphi}{2\pi}\{S_0\sigma_0 + [S_1 \sin(2\varphi) + S_3 \cos(2\varphi)]\sigma_1\}, \tag{12}$$

where φ denotes the azimuth angle of the electron momentum in the transverse plane. For σ_0, σ_1, we use expressions exact in $Z\alpha$ and valid for ultrarelativistic particles [83,93,94]. In the following, we assume a head-on collision $[q^\mu = \omega(1,0,0,1)$, $k^\mu = \omega_L(1,0,0,-1)$, $\Lambda_1^\mu = (0,1,0,0)$, $\Lambda_2^\mu = (0,0,1,0)]$, and tungsten ($Z = 74$) as conversion material.

As the pair-production cross section is only sensitive to linear polarization [S_1 and S_3, see Eq. (12)], we conclude from Eq. (11) that we need to utilize circularly polarized probe photons (e.g., $S^{(0)} = \{1, 0, -1, 0\}$) in order to obtain probabilities which depend on $\delta\phi$ [rather than $(\delta\phi)^2$] if $|\delta\phi| \ll 1$ (see also [57,58]). Therefore, inverting the standard scheme by using circularly instead of linearly polarized probe photons is highly beneficial in the regime $|\delta\phi| \lesssim 0.1$.

From Eq. (11), we conclude that S_1 is sensitive to vacuum birefringence ($\delta\phi$), whereas S_3 depends on vacuum dichroism ($\delta\lambda$). To disentangle both effects, we introduce the following asymmetries:

$$R_B = \frac{(N_{\pi/4} + N_{5\pi/4}) - (N_{3\pi/4} + N_{7\pi/4})}{(N_{\pi/4} + N_{5\pi/4}) + (N_{3\pi/4} + N_{7\pi/4})},$$
$$R_D = \frac{(N_0 + N_\pi) - (N_{\pi/2} + N_{3\pi/2})}{(N_0 + N_\pi) + (N_{\pi/2} + N_{3\pi/2})}, \tag{13}$$

where N_{β_0} denotes the number of pairs detected in the azimuth angle range $\varphi \in (\beta_0 - \beta, \beta_0 + \beta)$ of the transverse plane, with β being specified below [see Fig. 3(b)]. The expectation values of R_B and R_D are given by [see Eq. (12)]

$$\langle R_B \rangle = \frac{\sin(2\beta)}{2\beta}\frac{\sigma_1}{\sigma_0}\frac{S_1}{S_0}, \qquad \langle R_D \rangle = \frac{\sin(2\beta)}{2\beta}\frac{\sigma_1}{\sigma_0}\frac{S_3}{S_0}. \tag{14}$$

In order to detect vacuum birefringence (dichroism) at the $n\sigma$ confidence level on average, we require that the expectation value $\langle R_B \rangle$ ($\langle R_D \rangle$) differs from zero by n standard deviations. Therefore, we obtain the following expressions for the number of required incoming gamma photons (see Supplemental Material [83]):

$$N_\gamma^B = \frac{\pi n^2}{4\eta\beta S_0 \langle R_B \rangle^2}, \qquad N_\gamma^D = \frac{\pi n^2}{4\eta\beta S_0 \langle R_D \rangle^2} \tag{15}$$

TABLE I. Duration of the experiment τ at different facilities ($\chi = 0.25$). S_0 and S_1, $\langle R_B \rangle$, and N_γ^B follow from Eq. (11), Eq. (14) and Eq. (15), respectively ($S^{(0)} = \{1, 0, -1, 0\}$; 5σ confidence level, i.e., $n = 5$). Note that the pair production probability in the strong laser field is much smaller than the conversion efficiency in the detector [$(1 - S_0) \ll \eta = 10^{-2}$].

	$1 - S_0$	S_1	$\langle R_B \rangle$	N_γ^B	τ
Apollon	1.9×10^{-5}	0.06	3.4×10^{-3}	3.0×10^8	45 d
ELI-NP	3.1×10^{-5}	0.09	5.6×10^{-3}	1.1×10^8	10 d
ELI-BL	6.3×10^{-5}	0.18	1.1×10^{-2}	2.6×10^7	11 h
LINAC-L	3.8×10^{-6}	0.01	6.8×10^{-4}	7.4×10^9	2 d

[by minimizing N_γ^B (N_γ^D), we find the optimal angle $\beta = \beta_{opt} \approx 0.58 \approx 33°$ for both observables]. Here, $\eta = n_z l \sigma_0$ denotes the photon to pair conversion efficiency (n_z and l are the number density and the thickness of the conversion material, respectively). The thickness of a conversion foil should be $\lesssim 1$ milliradiation length (mRL), otherwise multiple Coulomb scattering affects the measured angle [91,93]. Supposing that several conversion foils alternating with silicon detectors are cascaded [95–97], we assume here $\eta = 10^{-2}$ (i.e., an effective thickness of ~10 mRL).

To obtain a clean vacuum birefringence experiment without real electron-positron pair production, we consider the case $\chi = 0.25$. The results for the four facilities under consideration are summarized in Table I. As expected from Fig. 4, ELI-Beamlines is the most suitable facility for carrying out the measurement in this regime (the expected measurement time is less than one day).

As the number of required gamma photons N_γ^B scales as $\langle R_B \rangle^{-2}$ [see Eq. (15)], the use of circularly polarized probe photons instead of linearly polarized ones reduces the measurement time by a factor ≈100 ($\delta\phi \approx 0.1$, see Fig. 4).

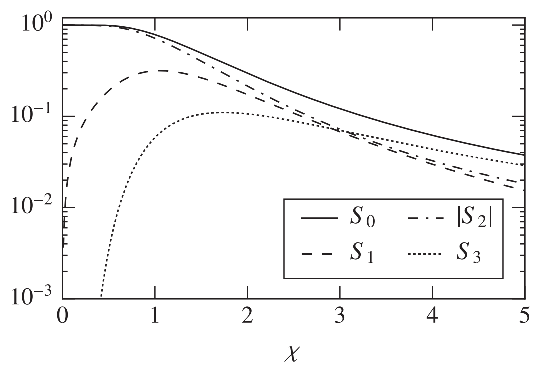

FIG. 5. Final Stokes parameters [see Eq. (11)] for gamma photons propagating through an ELI-NP 10 PW laser pulse ($S^{(0)} = \{1, 0, -1, 0\}$). The strongest effect is obtained around $\chi = 1$ (note that pair production becomes sizable for $\chi \gtrsim 1$). As we consider the tunneling regime $1/\xi \ll 1$, cusplike structures—characteristic for multiphoton pair production [18,65]—are absent.

Finally, we consider the case $\chi = 2.5$ (attainable, e.g., at ELI-NP by utilizing 8.4 GeV electrons for backscattering; $\theta_{\max} = 7.6 \times 10^{-6}$, $\sigma_{\mathrm{bs}} = 0.135 r_e^2$, $\omega = 1.4$ GeV, $\sigma_1/\sigma_0 = 0.077$; $r_e = \alpha/m = 2.818 \times 10^{-13}$ cm is the classical electron radius). In this regime, vacuum dichroism and anomalous dispersion come into play and the Euler-Heisenberg approximation breaks down completely (see Fig. 4), whereas the production of particles, heavier than electrons and positrons, and QCD corrections are still suppressed [98]. As the produced pairs radiate gamma photons, a discrimination of primary from secondary photons is necessary, e.g., via determination of the photon energy. For $S^{(0)} = \{1, 0, -1, 0\}$, we obtain that $S = \{0.18, 0.11, -0.12, 0.09\}$ at ELI-NP (see Fig. 5). Correspondingly, $\langle R_B \rangle = 3.6 \times 10^{-2}$ and $\langle R_D \rangle = 3.0 \times 10^{-2}$, implying a measurement time of 3-4 days [5σ confidence level, see Eq. (15)].

We would like to thank Oleg Skoromnik for useful discussions and Silvia Masciocchi for useful comments on the detection of gamma photons. S. M. was partially supported by the German Research Foundation (Deutsche Forschungsgemeinschaft, DFG)–ME 4944/1-1.

*s.meuren@mpi-hd.mpg.de; now at the Department of Astrophysical Sciences, Princeton University, Princeton, New Jersey 08544, USA.

[1] L. D. Landau and E. M. Lifshitz, *The Classical Theory of Fields*, 4th ed (Elsevier, Oxford, England, 1987).
[2] V. B. Berestetskii, E. M. Lifshitz, and L. P. Pitaevskii, *Quantum Electrodynamics*, 2nd ed (Elsevier, Oxford, England, 1982).
[3] G. V. Dunne, The Heisenberg-Euler effective action: 75 years on, Int. J. Mod. Phys. A **27**, 1260004 (2012).
[4] W. Dittrich and H. Gies, *Probing the Quantum Vacuum* (Springer, Berlin, Heidelberg, 2000).
[5] J. Schwinger, On gauge invariance and vacuum polarization, Phys. Rev. **82**, 664 (1951).
[6] W. Heisenberg and H. Euler, Folgerungen aus der Diracschen Theorie des Positrons, Z. Phys. **98**, 714 (1936).
[7] B. King and T. Heinzl, Measuring vacuum polarization with high-power lasers, High Power Laser Sci. Eng. **4**, e5 (2016).
[8] R. Battesti and C. Rizzo, Magnetic and electric properties of a quantum vacuum, Rep. Prog. Phys. **76**, 016401 (2013).
[9] A. Di Piazza, C. Müller, K. Z. Hatsagortsyan, and C. H. Keitel, Extremely high-intensity laser interactions with fundamental quantum systems, Rev. Mod. Phys. **84**, 1177 (2012).
[10] M. Marklund and P. K. Shukla, Nonlinear collective effects in photon-photon and photon-plasma interactions, Rev. Mod. Phys. **78**, 591 (2006).
[11] V. I. Ritus, Quantum effects of the interaction of elementary particles with an intense electromagnetic field, J. Sov. Laser Res. **6**, 497 (1985).
[12] H. Mitter, Quantum electrodynamics in laser fields, Acta Phys. Austriaca Suppl. **XIV**, 397 (1975).
[13] Here, $F^{\mu\nu}$ denotes the electromagnetic field tensor, $\tilde{F}^{\mu\nu} = \epsilon^{\mu\nu\sigma\tau} F_{\sigma\tau}/2$ is its dual, and $\epsilon^{\mu\nu\sigma\tau}$ is the totally antisymmetric pseudotensor. Heaviside and natural units are used ($\epsilon_0 = \hbar = c = 1$), i.e., the fine-structure constant is given by $\alpha = e^2/(4\pi) \approx 1/137$; and the metric tensor $g^{\mu\nu} = \mathrm{diag}(1, -1, -1, -1)$ is employed (m and $e < 0$ denote the electron mass and charge, respectively).
[14] Z. Bialynicka-Birula and I. Bialynicki-Birula, Nonlinear Effects in Quantum Electrodynamics, Photon Propagation and Photon Splitting in an External Field, Phys. Rev. D **2**, 2341 (1970).
[15] R. Baier and P. Breitenlohner, Photon propagation in external fields, Acta Phys. Austriaca **25**, 212 (1967).
[16] J. J. Klein and B. P. Nigam, Birefringence of the vacuum, Phys. Rev. **135**, B1279 (1964).
[17] J. S. Toll, Ph.D. thesis, Princeton University, 1952 (unpublished).
[18] S. Villalba-Chávez, S. Meuren, and C. Müller, Minicharged particles search by strong laser pulse-induced vacuum polarization effects, Phys. Lett. B **763**, 445 (2016).
[19] S. Villalba-Chávez and A. Di Piazza, Axion-induced birefringence effects in laser driven nonlinear vacuum interaction, J. High Energy Phys. 11 (2013) 136.
[20] D. Tommasini, A. Ferrando, H. Michinel, and M. Seco, Precision tests of QED and non-standard models by searching photon-photon scattering in vacuum with high power lasers, J. High Energy Phys. 11 (2009) 043.
[21] S. A. Abel, J. Jaeckel, V. V. Khoze, and A. Ringwald, Illuminating the hidden sector of string theory by shining light through a magnetic field, Phys. Lett. B **666**, 66 (2008).
[22] H. Gies, J. Jaeckel, and A. Ringwald, Polarized Light Propagating in a Magnetic Field as a Probe for Millicharged Fermions, Phys. Rev. Lett. **97**, 140402 (2006).
[23] J. Jaeckel and M. Spannowsky, Probing MeV to 90 GeV axion-like particles with LEP and LHC, Phys. Lett. B **753**, 482 (2016).
[24] J. Jaeckel and A. Ringwald, The Low-Energy Frontier of Particle Physics, Annu. Rev. Nucl. Part. Sci. **60**, 405 (2010).
[25] R. P. Mignani, V. Testa, D. González Caniulef, R. Taverna, R. Turolla, S. Zane, and K. Wu, Evidence for vacuum birefringence from the first optical-polarimetry measurement of the isolated neutron star RX J1856.5–3754, Mon. Not. R. Astron. Soc. **465**, 492 (2017).
[26] L. M. Capparelli, A. Damiano, L. Maiani, and A. D. Polosa, A note on polarized light from magnetars, Eur. Phys. J. C **77**, 754 (2017).
[27] R. Turolla, S. Zane, R. Taverna, D. González Caniulef, R. P. Mignani, V. Testa, and K. Wu, A Comment on "A note on polarized light from Magnetars: QED effects and axion-like particles" by L.M. Capparelli, L. Maiani and A.D. Polosa, arXiv:1706.02505.
[28] R. Cameron, G. Cantatore, A. C. Melissinos, G. Ruoso, Y. Semertzidis, H. J. Halama, D. M. Lazarus, A. G. Prodell, F. Nezrick, C. Rizzo, and E. Zavattini, Search for Nearly Massless, Weakly Coupled Particles by Optical Techniques, Phys. Rev. D **47**, 3707 (1993).
[29] A. Cadène, P. Berceau, M. Fouché, R. Battesti, and C. Rizzo, Vacuum magnetic linear birefringence using pulsed fields: Status of the BMV experiment, Eur. Phys. J. D **68**, 16 (2014).

[30] F. Della Valle, A. Ejlli, U. Gastaldi, G. Messineo, E. Milotti, R. Pengo, G. Ruoso, and G. Zavattini, The PVLAS experiment: Measuring vacuum magnetic birefringence and dichroism with a birefringent Fabry–Perot cavity, Eur. Phys. J. C **76**, 24 (2016).
[31] S.-J. Chen, H.-H. Mei, and W.-T. Ni, Q&A experiment to search for vacuum dichroism, pseudoscalar–photon interaction and millicharged fermions, Mod. Phys. Lett. A **22**, 2815 (2007).
[32] C. Danson, D. Hillier, N. Hopps, and D. Neely, Petawatt class lasers worldwide, High Power Laser Sci. Eng. **3**, e3 (2015).
[33] T. M. Jeong and J. Lee, Femtosecond petawatt laser, Ann. Phys. (Berlin) **526**, 157 (2014).
[34] S. Shakeri, S. Z. Kalantari, and S.-S. Xue, Polarization of a probe laser beam due to nonlinear QED effects, Phys. Rev. A **95**, 012108 (2017).
[35] H.-P. Schlenvoigt, T. Heinzl, U. Schramm, T. E. Cowan, and R. Sauerbrey, Detecting vacuum birefringence with x-ray free electron lasers and high-power optical lasers: A feasibility study, Phys. Scr. **91**, 023010 (2016).
[36] F. Karbstein and C. Sundqvist, Probing Vacuum Birefringence using X-Ray Free Electron and Optical High-Intensity Lasers, Phys. Rev. D **94**, 013004 (2016).
[37] G. Zavattini, F. Della Valle, A. Ejlli, and G. Ruoso, A polarisation modulation scheme for measuring vacuum magnetic birefringence with static fields, Eur. Phys. J. C **76**, 294 (2016).
[38] D. M. Tennant, Four Wave Mixing as a Probe of the Vacuum, Phys. Rev. D **93**, 125032 (2016).
[39] H. Gies, F. Karbstein, and N. Seegert, Quantum reflection of photons off spatio-temporal electromagnetic field inhomogeneities, New J. Phys. **17**, 043060 (2015).
[40] F. Fillion-Gourdeau, C. Lefebvre, and S. MacLean, Scheme for the detection of mixing processes in vacuum, Phys. Rev. A **91**, 031801 (2015).
[41] F. Karbstein and R. Shaisultanov, Photon Propagation in Slowly Varying Inhomogeneous Electromagnetic Fields, Phys. Rev. D **91**, 085027 (2015).
[42] H. Hu and J. Huang, Modified light-cone condition via vacuum polarization in a time-dependent field, Phys. Rev. A **90**, 062111 (2014).
[43] R. Mohammadi, I. Motie, and S.-S. Xue, Circular polarization from linearly-polarized-laser-beam collisions, Phys. Rev. A **89**, 062111 (2014).
[44] Y. Monden and R. Kodama, Interaction of two counter-propagating laser beams with vacuum, Phys. Rev. A **86**, 033810 (2012).
[45] B. King and C. H. Keitel, Photon–photon scattering in collisions of intense laser pulses, New J. Phys. **14**, 103002 (2012).
[46] G. Yu. Kryuchkyan and K. Z. Hatsagortsyan, Bragg Scattering of Light in Vacuum Structured by Strong Periodic Fields, Phys. Rev. Lett. **107**, 053604 (2011).
[47] K. Homma, D. Habs, and T. Tajima, Probing vacuum birefringence by phase-contrast Fourier imaging under fields of high-intensity lasers, Appl. Phys. B **104**, 769 (2011).
[48] B. King, A. Di Piazza, and C. H. Keitel, A matterless double slit, Nat. Photonics **4**, 92 (2010).
[49] D. Tommasini, A. Ferrando, H. Michinel, and M. Seco, Detecting photon-photon scattering in vacuum at exawatt lasers, Phys. Rev. A **77**, 042101 (2008).
[50] E. Lundström, G. Brodin, J. Lundin, M. Marklund, R. Bingham, J. Collier, J. T. Mendonça, and P. Norreys, Using High-Power Lasers for Detection of Elastic Photon-Photon Scattering, Phys. Rev. Lett. **96**, 083602 (2006).
[51] A. Di Piazza, K. Z. Hatsagortsyan, and C. H. Keitel, Light Diffraction by a Strong Standing Electromagnetic Wave, Phys. Rev. Lett. **97**, 083603 (2006).
[52] T. Heinzl, B. Liesfeld, K.-U. Amthor, H. Schwoerer, R. Sauerbrey, and A. Wipf, On the observation of vacuum birefringence, Opt. Commun. **267**, 318 (2006).
[53] B. King and N. Elkina, Vacuum birefringence in high-energy laser-electron collisions, Phys. Rev. A **94**, 062102 (2016).
[54] A. Ilderton and M. Marklund, Prospects for studying vacuum polarisation using dipole and synchrotron radiation, J. Plasma Phys. **82**, 655820201 (2016).
[55] Y. Nakamiya and K. Homma, Probing vacuum birefringence under a high-intensity laser field with gamma-ray polarimetry at the GeV scale, Phys. Rev. D **96**, 053002 (2017).
[56] V. Dinu, T. Heinzl, A. Ilderton, M. Marklund, and G. Torgrimsson, Vacuum refractive indices and helicity flip in strong-field QED, Phys. Rev. D **89**, 125003 (2014).
[57] T. N. Wistisen and U. I. Uggerhøj, Vacuum Birefringence by Compton Backscattering through a Strong Field, Phys. Rev. D **88**, 053009 (2013).
[58] G. Cantatore, F. Della Valle, E. Milotti, L. Dabrowski, and C. Rizzo, Proposed measurement of the vacuum birefringence induced by a magnetic field on high energy photons, Phys. Lett. B **265**, 418 (1991).
[59] N. Muramatsu, Y. Kon, S. Daté, Y. Ohashi, H. Akimune, J. Y. Chen, M. Fujiwara, S. Hasegawa, T. Hotta, T. Ishikawa, T. Iwata, Y. Kato, H. Kohri, T. Matsumura, T. Mibe *et al.*, Development of high intensity laser-electron photon beams up to 2.9 GeV at the SPring-8 LEPS beamline, Nucl. Instrum. Methods Phys. Res., Sect. A **737**, 184 (2014).
[60] H. R. Weller, M. W. Ahmed, H. Gao, W. Tornow, Y. K. Wu, M. Gai, and R. Miskimen, Research opportunities at the upgraded HIγS facility, Prog. Part. Nucl. Phys. **62**, 257 (2009).
[61] M. Fukuda, T. Aoki, K. Dobashi, T. Hirose, T. Iimura, Y. Kurihara, T. Okugi, T. Omori, I. Sakai, J. Urakawa, and M. Washio, Polarimetry of Short-Pulse Gamma Rays Produced through Inverse Compton Scattering of Circularly Polarized Laser Beams, Phys. Rev. Lett. **91**, 164801 (2003).
[62] I. F. Ginzburg, G. L. Kotkin, S. L. Panfil, V. G. Serbo, and V. I. Telnov, Colliding γe and $\gamma\gamma$ beams based on single-pass e^+e^- accelerators II. Polarization effects, monochromatization improvement, Nucl. Instrum. Methods Phys. Res. **219**, 5 (1984).
[63] T. Heinzl and A. Ilderton, Exploring high-intensity QED at ELI, Eur. Phys. J. D **55**, 359 (2009).
[64] V. N. Baier, A. I. Milstein, and V. M. Strakhovenko, Interaction between a photon and an intense electromagnetic wave, Sov. Phys. JETP **42**, 961 (1976).
[65] W. Becker and H. Mitter, Vacuum polarization in laser fields, J. Phys. A **8**, 1638 (1975).

[66] So far, the case of circularly polarized photons has only been discussed for proposals to measure vacuum birefringence in magnetic fields at $\chi \ll 1$ [57,58].
[67] S. Meuren, K. Z. Hatsagortsyan, C. H. Keitel, and A. Di Piazza, Polarization-operator approach to pair creation in short laser pulses, Phys. Rev. D **91**, 013009 (2015).
[68] S. Meuren, K. Z. Hatsagortsyan, C. H. Keitel, and A. Di Piazza, High-Energy Recollision Processes of Laser-Generated Electron-Positron Pairs, Phys. Rev. Lett. **114**, 143201 (2015).
[69] S. Meuren, C. H. Keitel, and A. Di Piazza, Polarization operator for plane-wave background fields, Phys. Rev. D **88**, 013007 (2013).
[70] *NIST Handbook of Mathematical Functions*, edited by F. W. J. Olver, D. W. Lozier, R. F. Boisvert, and C. W. Clark (Cambridge University Press, New York, 2010).
[71] S. Meuren, C. H. Keitel, and A. Di Piazza, Semiclassical picture for electron-positron photoproduction in strong laser fields, Phys. Rev. D **93**, 085028 (2016).
[72] K. Blum, *Density Matrix Theory and Applications*, 3rd ed (Springer, Berlin, Heidelberg, 2012).
[73] M. Born and E. Wolf, *Principles of Optics: Electromagnetic Theory of Propagation, Interference and Diffraction of Light*, 7th ed (Cambridge University Press, Cambridge, England, 1999).
[74] D. N. Papadopoulos, J. P. Zou, C. Le Blanc, G. Chériaux, P. Georges, F. Druon, G. Mennerat, P. Ramirez, L. Martin, A. Fréneaux, A. Beluze, N. Lebas, P. Monot, F. Mathieu, and P. Audebert, The Apollon 10 PW laser: Experimental and theoretical investigation of the temporal characteristics, High Power Laser Sci. Eng. **4**, e34 (2016).
[75] F. Negoita, M. Roth, P. G. Thirolf, S. Tudisco, F. Hannachi, S. Moustaizis, I. Pomerantz, P. Mckenna, J. Fuchs, K. Sphor, G. Acbas, A. Anzalone, P. Audebert, S. Balascuta, F. Cappuzzello *et al.*, Laser driven nuclear physics at ELI-NP, Rom. Rep. Phys. **68**, S37 (2016).
[76] I. C. E. Turcu, F. Negoita, D. A. Jaroszynski, P. Mckenna, S. Balascuta, D. Ursescu, I. Dancus, M. O. Cernaianu, M. V. Tataru, P. Ghenuche, D. Stutman, A. Boianu, M. Risca, M. Toma, C. Petcu *et al.*, High field physics and QED experiments at ELI-NP, Rom. Rep. Phys. **68**, S145 (2016).
[77] B. Rus, P. Bakule, D. Kramer, G. Korn, J. T. Green, J. Nóvak, M. Fibrich, F. Batysta, J. Thoma, J. Naylon, T. Mazanec, M. Vítek, R. Barros, E. Koutris, J. Hřebíček *et al.*, ELI-Beamlines laser systems: Status and design options, Proc. SPIE Int. Soc. Opt. Eng. **8780**, 87801T (2013).
[78] W. P. Leemans, A. J. Gonsalves, H.-S. Mao, K. Nakamura, C. Benedetti, C. B. Schroeder, Cs. Tóth, J. Daniels, D. E. Mittelberger, S. S. Bulanov, J.-L. Vay, C. G. R. Geddes, and E. Esarey, Multi-GeV Electron Beams from Capillary-Discharge-Guided Subpetawatt Laser Pulses in the Self-Trapping Regime, Phys. Rev. Lett. **113**, 245002 (2014).
[79] X. Wang, R. Zgadzaj, N. Fazel, Z. Li, S. A. Yi, X. Zhang, W. Henderson, Y.-Y. Chang, R. Korzekwa, H.-E. Tsai, C.-H. Pai, H. Quevedo, G. Dyer, E. Gaul, M. Martinez *et al.*, Quasi-monoenergetic laser-plasma acceleration of electrons to 2 GeV, Nat. Commun. **4**, 1988 (2013).
[80] European XFEL facility, https://www.xfel.eu.
[81] FACET-II Project, https://portal.slac.stanford.edu/sites/ard_public/facet/Pages/FACET-II.aspx.
[82] M. Yabashi, H. Tanaka, and T. Ishikawa, Overview of the SACLA facility, J. Synchrotron Radiat. **22**, 477 (2015).
[83] See Supplemental Material at http://link.aps.org/supplemental/10.1103/PhysRevLett.119.250403 for technical details, which includes Refs. [84–90].
[84] A. I. Akhiezer and V. B. Berestetskii, *Quantum Electrodynamics [In Russian]* (Nauka, Moscow, 1969).
[85] B. Le Garrec, S. Sebban, D. Margarone, M. Precek, S. Weber, O. Klimo, G. Korn, and B. Rus, ELI-beamlines: Extreme light infrastructure science and technology with ultra-intense lasers, Proc. SPIE Int. Soc. Opt. Eng. **8962**, 89620I (2014).
[86] ELI-Beamlines Lasers website, https://www.eli-beams.eu/en/facility/lasers/.
[87] Y.-S. Tsai, Pair production and bremsstrahlung of charged leptons, Rev. Mod. Phys. **46**, 815 (1974).
[88] K. F. Riley, M. P. Hobson, and S. J. Bence, *Mathematical Methods for Physics and Engineering*, 3rd ed (Cambridge University Press, Cambridge, England, 2006).
[89] F. James, *Statistical Methods in Experimental Physics*, 2nd ed (World Scientific, Singapore, 2006).
[90] H. H. Ku, Notes on the use of propagation of error formulas, J. Res. Natl. Bur. Stand., Sect. C **70C**, 263 (1966).
[91] S. D. Hunter, P. F. Bloser, G. O. Depaola, M. P. Dion, G. A. DeNolfo, A. Hanu, M. Iparraguirre, J. Legere, F. Longo, M. L. McConnell, S. F. Nowicki, J. M. Ryan, S. Son, and F. W. Stecker, A pair production telescope for medium-energy gamma-ray polarimetry, Astropart. Phys. **59**, 18 (2014).
[92] D. Bernard, Polarimetry of cosmic gamma-ray sources above e^+e^- pair creation threshold, Nucl. Instrum. Methods Phys. Res., Sect. A **729**, 765 (2013).
[93] S. R. Kelner, Yu. D. Kotov, and V. M. Logunov, Methods of measuring linear polarization of gamma quanta, Sov. J. Nucl. Phys. **21**, 313 (1975).
[94] H. Olsen and L. C. Maximon, Photon and electron polarization in high-energy bremsstrahlung and pair production with screening, Phys. Rev. **114**, 887 (1959).
[95] T. Peitzmann, Prototype studies for a forward EM calorimeter in ALICE, arXiv:1308.2585.
[96] W. B. Atwood, A. A. Abdo, M. Ackermann, W. Althouse, B. Anderson, M. Axelsson, L. Baldini, J. Ballet, D. L. Band, G. Barbiellini, J. Bartelt, D. Bastieri, B. M. Baughman, K. Bechtol, D. Bédérède *et al.* (Fermi Collaboration), The large area telescope on the Fermi gamma-ray space telescope mission, Astrophys. J. **697**, 1071 (2009).
[97] M. Tavani, G. Barbiellini, A. Argan, N. Auricchio, A. R. Bernabeo, A. Bulgarelli, P. A. Caraveo, E. Celesti, A. Chen, V. Cocco, E. Costa, E. Del Monte, G. De Paris, G. Di Cocco, G. Fedel *et al.*, The AGILE instrument, Proc. SPIE Int. Soc. Opt. Eng. **4851**, 1151 (2003).
[98] Z. Bern, A. De Freitas, A. Ghinculov, H. Wong, and L. Dixon, QCD and QED corrections to light-by-light scattering, J. High Energy Phys. 11 (2001) 031.